

Magnetostatic bounds on stability of hopfions in bulk helimagnets

Konstantin L. Metlov

*^aGalkin Donetsk Institute for Physics and Engineering, R. Luxemburg
str. 72, Donetsk, 283048, Russian Federation*

Abstract

Magnetic hopfions are three-dimensional localized topological solitons in the volume of a magnet. In this work, starting with a classical free energy density of a helimagnet, an approximate variational model of hopfions is studied. The hopfion stability regions on the uniaxial anisotropy-external magnetic field phase diagram are computed and their evolution with increasing magnetostatic interaction strength is considered. It is found that magnetostatic interaction destabilizes the hopfions and, above the certain strength (relative to Dzyaloshinskii-Moriya interaction), destroys their stability completely. Numerical estimates for this bound are provided. They can help focus the search for materials, supporting bulk magnetic hopfions.

Keywords: micromagnetics, hopfions, helimagnet, magnetostatic energy
PACS: 75.70.Kw, 75.60.Ch, 74.25.Ha, 41.20.Gz

1. Introduction

Topology is a powerful tool for exploring the consequences of continuity. In our everyday observations of the physical world, continuity manifests itself as an evident gradual change of various physical quantities in space and time. Yet, as noticed in physics at least since lord Kelvin [1], it also leads to emergence of a rich discrete set of objects. These correspond to the subdivision of a set of continuous mappings into topological classes, with their elements equivalent up to another (family of continuous maps) – homotopy. The most ubiquitous example of these classes emerge during the classification of knots [2] on a rope.

Rope is one-dimensional, but higher-dimensional knots are also possible. In magnetism these manifest themselves in the form of two-dimensional

(2D) Belavin-Polyakov (BP) solitons [3] (the BP solitons in thin ferromagnetic films are known as magnetic bubbles [4], in bulk chiral magnets as skyrmions [5], and in magnetic dots with in-plane magnetostatic anisotropy as magnetic vortices [6] even though they are described by a slightly different set of solutions of the same model, called merons [7]), whose topological classification is the same as that of mappings between the surfaces of two spheres (denoted as $S^2 \rightarrow S^2$). The first of these two spheres corresponds to all the locations in a 2D ferromagnet with periodic boundary conditions at infinity and the second to the endpoints of the constant-length local magnetization vectors. Just like magnetization configurations around Bloch points [8], the BP solitons have a natural description in terms of functions of complex variable [3], which becomes especially useful in restricted planar geometry [7].

A natural generalization of BP solitons to three dimensions [9] is to consider magnetization states, corresponding to the mapping of three-dimensional surface of a four-dimensional hypersphere S^3 (volume of the magnet with periodic boundary conditions at infinity) onto the surface of S^2 sphere (endpoints of the magnetization vectors). For a long time in mathematics it was accepted that all such mappings are homotopically equivalent (and topologically trivial) until Heinz Hopf in 1931 provided an example [10] of a different (homotopically irreducible to the previously known) map. This example was generalized by Whitehead [11], who have shown that there is a number of such topologically non-trivial maps, characterized by an integer number – Hopf invariant (or Hopf index). The topological solitons, corresponding to these non-trivial $S^3 \rightarrow S^2$ maps, took a name of hopfions. As far as magnetic hopfions are concerned, there was an extensive published theoretical research (including books) on those in bulk magnets with complex/unusual exchange interactions [12, 13, 14] and systems with uniaxial anisotropy [15, 16, 17]. There is recently a substantial renewed interest to magnetic hopfions [18, 19], which produced several experimental realizations of magnetic hopfions (or parts of hopfions) in confined geometry [20, 21, 22].

Yet, only the hopfions in bulk magnets can fully realize unique potential of these topological objects for 3D spintronics and search for them still continues. These bulk hopfions are not easy to simulate numerically, because the amount of computational resources, necessary to fully simulate 3D magnets, scales much faster with system size (which must be reasonably high to simulate the bulk), compared to the extensively studied in simulations planar nanomagnets. The hopfions do appear in micromagnetic simulations (e.g. [19]), but analytical (or semianalytical) models are still better suited

for mapping the hopfions stability range on the magnetic phase diagrams.

Such a semianalytical model (but still based on classical micromagnetic Hamiltonian) was considered recently in [23]. It predicts the existence of two types of metastable magnetic hopfions in a bulk helimagnet. The present work reports a comprehensive study of the dependence of the hopfion stability region (for both types of hopfions) on the relative strength of the magnetostatic interaction. In the next section, the considered model is formally introduced, the corresponding magnetic energy terms are computed and presented in Appendices. In Section 3 numerically computed stability ranges of the hopfions are plotted and discussed. Section 4 concludes the study.

2. Model

As a starting point, consider the ansatz for an $S^3 \rightarrow S^2$ mapping with non-zero Hopf index

$$w = e^{i\chi} \frac{u^n}{v^k}, \quad (1)$$

where u and v are complex coordinates on a unit S^3 sphere, satisfying the constraints $|u|^2 + |v|^2 = 1$; n and k are two mutually prime integers; and w is the coordinate on the target S^2 sphere, so that the components of the normalized magnetization vector $\mathbf{m} = \mathbf{M}/M_S$ are

$$\{m_X + im_Y, m_Z\} = \{2w, 1 - |w|^2\}/(1 + |w|^2). \quad (2)$$

The Hopf index of the resulting map is $\mathcal{H} = nk$, but we will limit ourselves here only to the simplest $\mathcal{H} = n = k = 1$ case. The real parameter χ does not influence the topology and (1) coincides with the Whitehead's ansatz [11] when $\chi = 0$. Yet, the energy analysis [23], based on a classical micromagnetic Hamiltonian (including most notably the Dzyaloshinskii-Moriya and the magnetostatic energy terms), shows that χ takes one of two stable equilibrium values: $\chi = \pi/2$ and $\chi = 3\pi/2$. These values correspond to type I and type II hopfions, respectively.

The coordinates on the sphere S^3 can be specified in terms of the coordinates of a point $\tilde{X}, \tilde{Y}, \tilde{Z}$ on the extended Euclidean space E^3 (with implied periodic boundary conditions at infinity)

$$u = \frac{2(\tilde{X} + i\tilde{Y})R}{\tilde{X}^2 + \tilde{Y}^2 + \tilde{Z}^2 + R^2}, \quad v = \frac{R^2 - \tilde{X}^2 - \tilde{Y}^2 - \tilde{Z}^2 + i2\tilde{Z}R}{\tilde{X}^2 + \tilde{Y}^2 + \tilde{Z}^2 + R^2}, \quad (3)$$

where R is a (yet unknown) spatial scale. One can see that the origin $\tilde{X} = \tilde{Y} = \tilde{Z} = 0$ is mapped onto $(u, v) = (0, 1)$ and the infinitely distant point in any direction $\tilde{X}, \tilde{Y}, \tilde{Z} \rightarrow \infty$ to $(u, v) = (0, -1)$. Both these points map to $w = 0$ and $\mathbf{m} = \{0, 0, 1\}$ directed along the OZ axis of the chosen Cartesian coordinate system. Finally, to map the coordinates of the physical X, Y, Z space onto E^3 we use

$$\{\tilde{X}, \tilde{Y}, \tilde{Z}\} = \frac{\{X, Y, Z\}}{1 - f(\sqrt{X^2 + Y^2 + Z^2}/R)}, \quad (4)$$

where $f(\rho)$, $0 \leq \rho \leq 1$ is a yet unknown function, satisfying the boundary conditions $f(0) = 0$, $f'(0) = 0$, $f(1) = 1$. This ensures that the hopfion is strongly localized inside the ball of the radius R , whose boundary $X^2 + Y^2 + Z^2 = R^2$ is mapped to the infinitely distant point $\tilde{X}, \tilde{Y}, \tilde{Z} \rightarrow \infty$ in E^3 . In the framework of this Ritz-type model, finding stable hopfions means finding the value of the scalar parameter R and the profile of the function $f(\rho)$, minimizing the Hamiltonian of the physical model, expressed in terms of the vector \mathbf{m} of the fixed length $|\mathbf{m}| = 1$. Explicitly, the magnetization components inside the $\mathcal{H} = 1$ hopfion are given in the Appendix A and shown in Fig. 1.

Note that only the last equation (4) carries the model assumptions here. This is because all the hopfions with the same \mathcal{H} are equivalent up to a continuous map (homotopy). A sufficiently general map from X, Y, Z to $\tilde{X}, \tilde{Y}, \tilde{Z}$ together with eqs. (1) to (3) is able to describe the exact hopfion solutions of a considered physical model Hamiltonian (not even necessarily micromagnetic). Limiting the minimization to a specific subset of the maps (4) simplifies the consideration, but makes the resulting hopfion profiles only approximate.

The map (4) is sufficient [23] to obtain stable hopfion solutions for the classical micromagnetic free energy density

$$e = \frac{C}{2} \sum_{i=X,Y,Z} |\nabla m_i|^2 + D \mathbf{m} \cdot [\nabla \times \mathbf{m}] - \mu_0 M_S (\mathbf{m} \cdot \mathbf{H}) - \frac{\mu_0 M_S}{2} (\mathbf{m} \cdot \mathbf{H}_D) - K (\mathbf{m} \cdot \mathbf{s})^2, \quad (5)$$

where $C = 2A$ is the exchange stiffness, D is the Dzyaloshinskii-Moriya interaction strength [24, 25], \mathbf{H} is the external magnetic field, \mathbf{H}_D is the demagnetizing field, created by all the magnetic moments in the material as

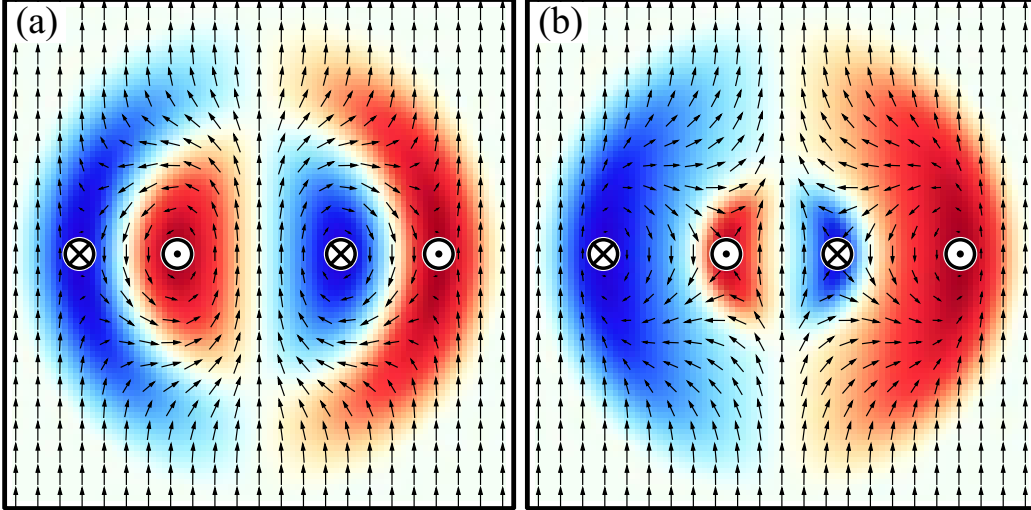


Figure 1: Magnetization distributions inside the equilibrium type I (a) and type II (b) hopfions when no field or anisotropy is present ($h = q = 0$) and the magnetostatic parameter $\mu = 1/3$; the shading and circular symbols show the the out-of-plane magnetization component; the equilibrium size parameters in this case are $\nu^I \approx -0.199894$ and $\nu^{II} \approx 0.099267$, so that the type II hopfion is roughly twice the size of the type I hopfion.

per Maxwell's equations, K and \mathbf{s} are the uniaxial anisotropy constant and director. Following Aharoni [26], the relation $\mathbf{B} = \mu_0(\mathbf{H} + \gamma_B \mathbf{M})$ for the magnetic induction allows us to cover all the common systems of magnetic units [μ_0 is the permeability of vacuum and $\gamma_B = 1$ in SI; $\gamma_B = 4\pi$, $\mu_0 = 1$ in CGS]. In the present consideration we will assume that the direction of the external field $\mathbf{H} = \{0, 0, H\}$ and the anisotropy axis director $\mathbf{s} = \{0, 0, 1\}$ coincide with the hopfion axis lying along the OZ axis of the Cartesian coordinate system we use. In this system, according to eqs. (1) to (4), the magnetization along the axis of the hopfion $X = Y = 0$ on its spherical boundary and outside is $\mathbf{m} = \{0, 0, 1\}$.

Assuming (as in [23]) the hopfions are arranged in a close-packed lattice, its total energy $E = (1/V) \iiint_V e d^3\mathbf{r}$ per unit cell volume V in dimensionless

units $\epsilon = EC/D^2$ can be expressed as a functional $\epsilon = \int_0^1 F d\rho$ with

$$F = \frac{1}{4\sqrt{2}} \left(\nu^2 P_{\text{EX}} + \nu P_{\text{DM}} + \frac{q}{2} (P_{\text{A}} - 4\sqrt{2}) + h(P_{\text{Z}} - 4\sqrt{2}) + \mu^2 P_{\text{MS}} \right), \quad (6)$$

where $4\sqrt{2}R^3$ is the volume per hopfion inside the unit cell of the close packed lattice, $\nu = C/(DR)$ is the dimensionless size parameter, inversely proportional to the hopfion radius R , $h = \mu_0 M_S CH/D^2$ is the normalized external field, $q = 2CK/D^2$ normalized anisotropy quality factor, $\mu^2 = \mu_0 \gamma_B M_S^2 C/D^2$ is the dimensionless magnetostatic interaction strength parameter (μ^2 is also known as the susceptibility of the conical helix [27]) and the energy functions

$$P_i = \int_0^{2\pi} d\varphi \int_0^\pi d\theta p_i \rho^2 \sin \theta \quad (7)$$

with $p_{\text{EX}} = (R^2/2) \sum_{i=X,Y,Z} |\nabla m_i|^2$, $p_{\text{DM}} = R \mathbf{m} \cdot [\nabla \times \mathbf{m}]$, $p_{\text{A}} = 1 - m_Z^2$, $p_{\text{Z}} = 1 - m_Z$, while p_{MS} is itself defined via the integral over ρ due to non-locality of the dipolar energy. For both types of hopfions, the angular integrals in (7) can be evaluated analytically. The expressions for P_i are given in the Appendix B. They depend on ρ , the hopfion profile function $f(\rho)$ and its derivative $f'(\rho)$.

The problem for finding the equilibrium $f(\rho)$ then reduces to solving the Euler-Lagrange equation

$$\frac{\partial F}{\partial f} - \frac{\partial}{\partial \rho} \frac{\partial F}{\partial f'} = 0. \quad (8)$$

In our case, it is a second order differential equation, requiring two boundary/initial conditions to solve. There is also an unknown scalar parameter ν , which needs to be chosen in such a way that all three initial/boundary conditions

$$f(0) = 0, \quad f'(0) = 0, \quad f(1) = 1 \quad (9)$$

are satisfied. This can be implemented by making ν a function $\nu(\rho)$ and adding another equation:

$$\nu'(\rho) = 0. \quad (10)$$

Together with (8) we get a system of three first order differential equations for $f(\rho)$, $f'(\rho)$ and $\nu(\rho)$. Three initial/boundary conditions (9) make this problem well defined. It can be solved numerically using the method of shooting. Here this was done with MUS [28].

Non-locality of magnetostatic interaction poses another problem by adding an integral term to the Euler equation (8). It was handled using an iterative scheme. When solving the boundary value problem in eqs. (8) to (10) for $f_n(\rho)$ on the n -th iteration, the magnetostatic functions W_1 , V_1 , V_2 (see the Appendix B) are evaluated, based on the previous iteration $f_{n-1}(\rho)$. This removes the integral term from the equation, replacing it by an integral of the known previous-iteration function. The calculation is then repeated until the changes between the hopfion profile on successive iterations become negligible. Once the convergence is achieved, the resulting hopfion profile solves the full integro-differential Euler-Lagrange equation.

3. Results and discussion

There are two instabilities, embedded into the considered model: hopfions may be unstable with respect to the collapse of their size to zero $\nu \rightarrow \infty$ or to the expansion to infinity $\nu \rightarrow 0$. In either case the method of shooting fails to find the solution for $f(\rho)$, satisfying the boundary conditions (9). If the magnetostatic interaction is included, near the stability boundary the iterations for finding the $f(\rho)$, satisfying the integro-differential Euler equation, may not converge to the true solution and instead loop around it (in such situation we also consider the solution to be unstable).

The process of tracing the stability boundary starts at a certain point of the q - h phase diagram for a particular value of μ , such that the hopfion solution at this point exists and is stable. Next step is to move in an arbitrary direction in small and gradually decreasing steps, using the previous $f(\rho)$ and ν as initial guess for the solution in the next point, until the solution becomes unstable. This means the stability boundary is reached. Next, the tracer follows the boundary, keeping it always on a right (or left) side of its current position until a full circle is made. The result is a complete stability line on the phase diagram. This procedure (together with computation of the equilibrium hopfion profile, described in the previous section) is implemented in Fortran programming language and published as a GitHub repository under the project name `magnhopf` [29].

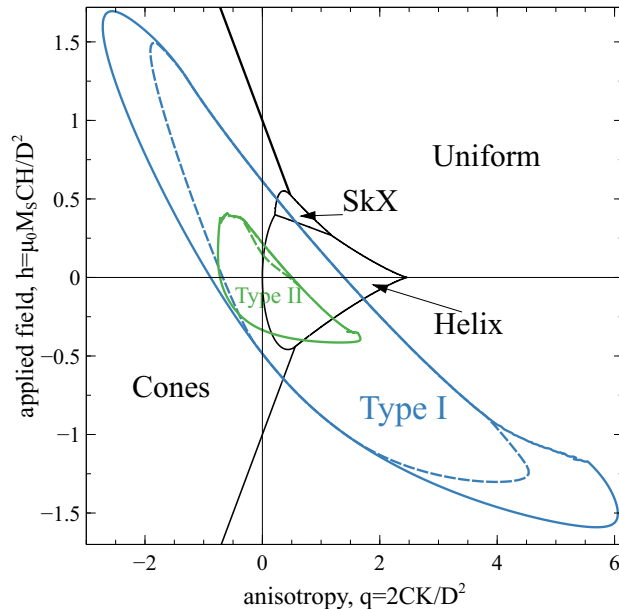


Figure 2: Theoretical stability regions of the type I and type II hopfions when the magnetostatic interaction is neglected ($\mu^2 = 0$), superimposed over the ground state diagram of the helimagnet with uniform, conical, helical, and skyrmion lattice phase [30, 31]. The dashed lines separate the hopfion states with monotonous and non-monotonous $f(\rho)$.

The resulting stability regions on the q - h plane when the magnetostatic interaction is negligible ($\mu = 0$) are shown in Fig. 2. Due to the approximate nature of the performed search, there is no guarantee that the true stability boundary is found this way. The strong statement is that anywhere inside this stability boundary the above-described numerical procedure can always obtain a stable hopfion solution with a particular hopfion profile $f(\rho)$ and a hopfion size parameter ν . Improvement in the numerical procedure, such as increasing the search resolution, might move the stability lines somewhat. Nevertheless, our numerical experiments (with different resolutions and other numerical parameters) do not show that this dependence is significant and the resulting fluctuations on the stability lines are small.

Compared to Fig. 2 in [23], this diagram covers also negative values of the quality factor and the external field, fully outlining the stability regions of hopfions. One can see from the superimposed ground state diagrams that (meta) stable hopfions exist roughly at the same range of material parameters

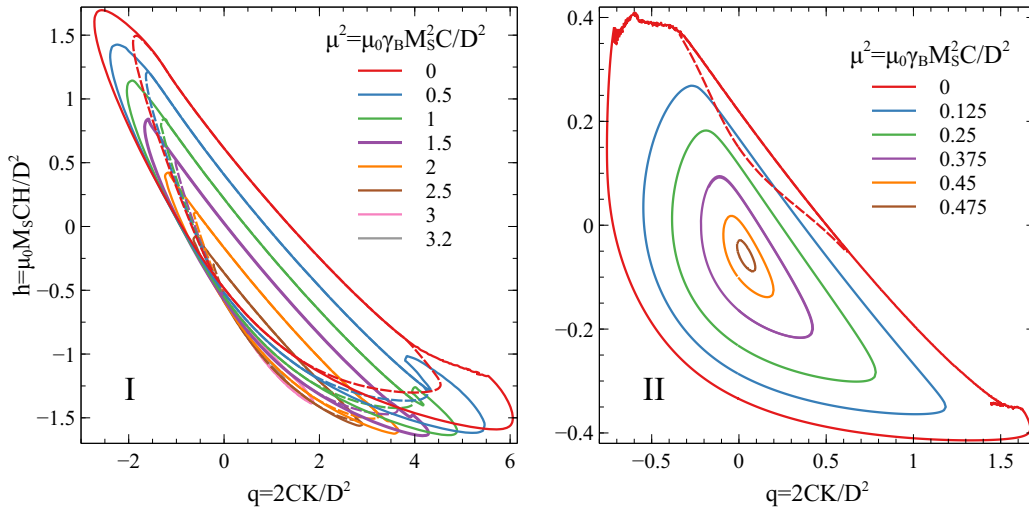


Figure 3: Evolution of stability regions of the type I (left) and type II (right) hopfions as the magnetostatic interaction strength parameter μ^2 increases.

as the skyrmions and other well known phases of helimagnet.

In [23] it was already noted that the equilibrium hopfion profile $f(\rho)$ is not always monotonous. This is not a problem, since a hopfion with a non-monotonous $f(\rho)$ can be transformed into a one with monotonous profile via a homotopy, meaning that non-monotonicity does not change the topological class. Nevertheless, in Fig. 2 and Fig. 3 the subset of hopfion states with monotonous profiles is additionally outlined with the dashed line. This subset for both hopfion types is located on top (larger field side) of each stability region and for the type II hopfions at $\mu^2 = 0$ it is very small. For larger μ^2 a subset of type II hopfions with monotonous $f(\rho)$ quickly vanishes, it was impossible to find already for $\mu^2 \geq 0.125$ in the present numerical calculations.

Dependence of the hopfion stability regions on the magnetostatic interaction strength μ^2 is shown in Fig. 3. The main feature on these plots is that the stability region progressively shrinks (in the case of type I hopfions it also shifts towards the smaller/negative fields) as the magnetostatic interaction strength increases. It means that the magnetostatic interaction suppresses the hopfion state.

It is interesting to note in context of a known theoretical result [32, 33]

Material	μ^2	T_C , K
MnSi	0.34	29
Cu ₂ OSeO ₃	1.76	58
Fe _{0.8} Co _{0.2} Si	0.65	28
FeGe	3.43	278

Table 1: Material parameters for some skyrmion hosting materials, collected in [27] from references therein.

that the magnetostatic interaction is able to stabilize the cross-tie domain wall in the limit of infinite film thickness (when it is just a linear sequence of alternating parallel infinite straight vortex and antivortex lines in the bulk of the magnet). Since the $\mathcal{H} = 1$ hopfion is just a vortex and an anti-vortex lines, woven on top of each other, the deciding factor seems to be the curvature of these lines. The straight nearby vortex and antivortex lines attract and form a bound state (the cross-tie wall) via the attraction of the volume magnetic charges of the opposite sign around them. But the circular vortex and antivortex lines in the hopfion produce more of the concentrated magnetic charges of the same sign, increasing magnetostatic energy up to a point that it becomes energetically favorable to remove the hopfion altogether. This is like in the case of the ordinary magnetic domain walls, which have associated area energy density. This energy disfavors the wall curvature and produces additional curvature-related pressure from the wall (like e.g. in the case of a circular domain wall of a magnetic bubble).

Whatever the mechanism, from the evolution of the stability regions in Fig. 3 it is possible to roughly estimate the limiting values of $3.2 < \mu_I^2 \lesssim 3.3$ and $0.475 < \mu_{II}^2 \lesssim 0.48$. At $\mu > \mu_I$ (for type I hopfions) and $\mu > \mu_{II}$ (for type II hopfions) the stability region completely vanishes and the hopfion state was impossible to stabilize in our computations. These numbers are in range of the parameters of well known chiral skyrmion hosting materials, shown in Table 1. It follows, for example, that the room temperature FeGe is unlikely to support the free standing bulk hopfions of any type. But other listed materials can support either type I hopfions or both (like MnSi) at cryogenic temperatures. Let us stress, that this limit concerns only the free standing hopfions in the bulk. Stabilization of hopfions in nanostructures [19] or observations of individual pairs of hopfions (like torons [21], which are just a single circular vortex line) are not subject to this particular limit.

It is important to realize that unlike other known states of helimagnet, such as spirals and helices (which have zero magnetostatic energy) or skyrmions (whose magnetostatic energy is negligible), the hopfions are strongly influenced by magnetostatic interaction and this influence is destabilizing. So, the ideal material to look for hopfions should have as small $\mu^2 = \mu_0 \gamma_B M_S^2 C / D^2$ as possible. Probably the most straightforward way to achieve this is via a competition of the sublattice magnetizations in a chiral ferrimagnet.

Finally, let us also stress that the precise numbers for the μ_I and μ_{II} above depend on the considered variational model and may change if the model is improved. Yet, it is beyond any doubts at this point that magnetostatic interaction makes the observation of free space hopfions harder.

4. Summary & Conclusions

A variational model for magnetic hopfions in a classical helimagnet is considered. Its energy terms, corresponding to the exchange, uniaxial anisotropy, external field, Dzyaloshinskii-Moriya (DM) interaction and the magnetostatic energy are computed and presented in the Appendix B. A program for finding the equilibrium hopfion profile, minimizing the corresponding energy functional, is developed [29]. This program allows to compute the full hopfion stability region on the anisotropy-external field phase diagram and study its dependence on the magnetostatic interaction strength to the DM interaction constant ratio μ^2 . It is shown that the magnetostatic interaction has destabilizing effect on hopfions. Moreover, there are certain limiting values of μ^2 , specific to each of the two hopfion types, such that for higher μ^2 the hopfion stability region on the phase diagram completely vanishes. These limiting values are estimated on the basis of the studied model and are discussed in context of the material parameters for certain well known model helimagnets. They can be useful to help narrow the search for stable bulk hopfions.

Appendix A. Hopfion magnetization in spherical coordinates

Because of the symmetry, the spherical coordinate system with a polar axis along the direction of the applied field (and the considered anisotropy) is natural for description of spherical hopfions. Starting from the connection between the Cartesian and spherical coordinates

$$\{X, Y, Z\} = \rho R \{\cos \varphi \sin \theta, \sin \varphi \sin \theta, \cos \theta\}, \quad (\text{A.1})$$

the transformation matrix, connecting the Cartesian and spherical vectorial components, consists of normalized (to have the unit length) rows of derivatives of the coordinate transforms (A.1) over ρ, θ, φ

$$\begin{bmatrix} m_\rho \\ m_\theta \\ m_\varphi \end{bmatrix} = \begin{bmatrix} \sin \theta \cos \varphi & \sin \theta \sin \varphi & \cos \theta \\ \cos \theta \cos \varphi & \cos \theta \sin \varphi & -\sin \theta \\ -\sin \varphi & \cos \varphi & 0 \end{bmatrix} \begin{bmatrix} m_X \\ m_Y \\ m_Z \end{bmatrix}. \quad (\text{A.2})$$

The Cartesian magnetization vector components $\{m_X, m_Y, m_Z\}$ can be computed from eqs. (1) to (4). The same vector field in the spherical coordinate system (A.1), (A.2) for hopfions of the first type ($\chi = \pi/2$) is

$$\{m_\rho^{\text{I}}, m_\theta^{\text{I}}, m_\varphi^{\text{I}}\} = \left\{ \cos \theta, -\frac{(g^4 - 6g^2\rho^2 + \rho^4) \sin \theta}{(g^2 + \rho^2)^2}, \frac{4g\rho(g^2 - \rho^2) \sin \theta}{(g^2 + \rho^2)^2} \right\} \quad (\text{A.3})$$

and for hopfions of the second type ($\chi = 3\pi/2$) is

$$\{m_\rho^{\text{II}}, m_\theta^{\text{II}}, m_\varphi^{\text{II}}\} = \left\{ \frac{4g^2\rho^2 \cos 3\theta + (g^2 - \rho^2)^2 \cos \theta}{(g^2 + \rho^2)^2}, -\sin \theta \left(1 + \frac{8g^2\rho^2 \cos 2\theta}{(g^2 + \rho^2)^2} \right), -\frac{4g\rho(g^2 - \rho^2) \sin \theta}{(g^2 + \rho^2)^2} \right\}, \quad (\text{A.4})$$

where $g = 1 - f(\rho)$. Evidently (because the vector field components do not depend on the azimuthal angle φ), the $\mathcal{H} = 1$ hopfions are axially symmetric. That is, their cross section by any plane, passing through the polar (OZ) coordinate system axis, will contain exactly the same distribution of in-plane and out-of-plane components of the magnetization vector.

Appendix B. Hopfion energy terms

The exchange term of the functional can be calculated directly from its definition, performing the angular integration. It is the same for type I and type II hopfions

$$P_{\text{EX}} = \frac{64\pi\rho^2 (3g^2 - 2g\rho g' + \rho^2 (g')^2)}{3(g^2 + \rho^2)^2}, \quad (\text{B.1})$$

where $g = g(\rho) = 1 - f(\rho)$ and $g' = g'(\rho) = -f'(\rho)$. This term depends on $\rho, f(\rho)$ and its derivative $f'(\rho)$.

The Zeeman and the anisotropy terms are also the same for both hopfion types and do not contain the derivative $f'(\rho)$

$$P_Z = \frac{64\pi g^2 \rho^4}{3(g^2 + \rho^2)^2}, \quad (\text{B.2})$$

$$P_A = \frac{128\pi g^2 \rho^4 (5g^4 - 6g^2 \rho^2 + 5\rho^4)}{15(g^2 + \rho^2)^4}. \quad (\text{B.3})$$

The Dzyaloshinskii-Moriya term can also be directly evaluated from the definition, but, unlike the previous terms, it is different for type I and type II hopfions

$$P_{\text{DM}}^{\text{I}} = -\frac{32\pi \rho^2 (-3g^3 + \rho(g^2 + \rho^2)g' + g\rho^2)}{3(g^2 + \rho^2)^2}, \quad (\text{B.4})$$

$$P_{\text{DM}}^{\text{II}} = \frac{32\pi \rho^2 (-15g^7 + 55g^5 \rho^2 - 53g^3 \rho^4 + 5g\rho^6)}{15(g^2 + \rho^2)^4} + \frac{32\pi \rho^3 (5g^4 - 6g^2 \rho^2 + 5\rho^4)g'}{15(g^2 + \rho^2)^3}. \quad (\text{B.5})$$

To compute the magnetostatic self-energy of the hopfion, first, we need to evaluate the density of its volume magnetic charges. This density is simply the divergence of the magnetization vector field (multiplied by R to make it dimensionless). For each of the hopfion types the density of charges is

$$\sigma^{\text{I}} = \frac{16g^2 \rho \cos \theta}{(g^2 + \rho^2)^2}, \quad (\text{B.6})$$

$$\sigma^{\text{II}} = -\frac{16g\rho(g^3 + 2\rho(\rho^2 - g^2)g' - 3g\rho^2)\cos \theta}{(g^2 + \rho^2)^3} + \frac{32g\rho^2((\rho^2 - g^2)g' - 2g\rho)\cos^3 \theta}{(g^2 + \rho^2)^3}. \quad (\text{B.7})$$

The magnetostatic self-energy is then

$$\frac{\epsilon_{\text{MS}}}{\mu^2} = \int_0^1 P_{\text{MS}} d\rho = \frac{1}{8\pi} \iiint_{|\rho|<1} d^3 \boldsymbol{\rho} \iiint_{|\rho'|<1} d^3 \boldsymbol{\rho}' \frac{\sigma(\boldsymbol{\rho})\sigma(\boldsymbol{\rho}')}{|\boldsymbol{\rho} - \boldsymbol{\rho}'|}, \quad (\text{B.8})$$

where the factor 1/2 is already taken into account and the integration is performed in dimensionless units. To factor this integral we shall use the

identity

$$\frac{1}{|\boldsymbol{\rho} - \boldsymbol{\rho}'|} = 4\pi \sum_{l=0}^{\infty} \frac{1}{2l+1} \frac{\rho_{\min}^l}{\rho_{\max}^{l+1}} \sum_{m=-\infty}^{\infty} Y_l^m(\theta, \varphi) \overline{Y_l^m(\theta', \varphi')}, \quad (\text{B.9})$$

where the spherical coordinates $\boldsymbol{\rho} = \{\rho, \theta, \varphi\}$, $\boldsymbol{\rho}' = \{\rho', \theta', \varphi'\}$ are used, $\rho_{\min} = \min(\rho, \rho')$, $\rho_{\max} = \max(\rho, \rho')$, $Y_l^m(\theta, \varphi)$ are the spherical harmonics and the overline denotes the complex conjugate. Note that for the type I hopfions, the sum in (B.9) contains only the $l = 1$ term, while for the hopfions of the type II $l = 1$ and $l = 3$ terms. Performing the angular integration, the magnetostatic energy term can be represented as

$$P_{\text{MS}}^{\text{I}} = \frac{64\pi g^2 \rho W_1(\rho, \{f\})}{9(g^2 + \rho^2)^2}, \quad (\text{B.10})$$

$$W_1 = \int_0^\rho d\rho \frac{16g^2 \rho^4}{(g^2 + \rho^2)^2}, \quad (\text{B.11})$$

$$P_{\text{MS}}^{\text{II}} = - \frac{64g((g^2 - \rho^2)g' + 2g\rho)V_1(\rho, \{f\})}{(g^2 + \rho^2)^3} - \frac{32g\rho(5g^3 + 4\rho(\rho^2 - g^2)g' - 3g\rho^2)V_2(\rho, \{f\})}{3(g^2 + \rho^2)^3}, \quad (\text{B.12})$$

$$V_1 = \int_0^\rho d\rho \frac{256\pi g \rho^7 ((\rho^2 - g^2)g' - 2g\rho)}{1225(g^2 + \rho^2)^3}, \quad (\text{B.13})$$

$$V_2 = \int_0^\rho d\rho \frac{32\pi g \rho^4 (3g\rho^2 - 5g^3 - 4\rho(\rho^2 - g^2)g')}{75(g^2 + \rho^2)^3}. \quad (\text{B.14})$$

The total normalized magnetostatic energy (B.8) depends only on the shape of the hopfion profile function $f(\rho)$. For a simple test case $f(\rho) = \rho^2$ the above expressions give $\epsilon_{\text{MS}}^{\text{I}}/\mu^2 = 0.854\,101\,633$ and $\epsilon_{\text{MS}}^{\text{II}}/\mu^2 = 0.774\,089\,652$. These values were also verified by direct numerical 6-fold integration of (B.8).

References

- [1] W. Thomson, 4. On Vortex Atoms, Proceedings of the Royal Society of Edinburgh 6 (1869) 94–105. doi:10.1017/S0370164600045430.
- [2] R. H. Crowell, R. H. Fox, Introduction to Knot Theory, Springer New York, 1977. doi:10.1007/978-1-4612-9935-6.

- [3] A. A. Belavin, A. M. Polyakov, Metastable states of two-dimensional isotropic ferromagnet., ZETP lett. 22 (10) (1975) 245–247.
- [4] A. H. Bobeck, E. Della Torre, Magnetic bubbles, North-Holland, Amsterdam, 1975.
- [5] U. K. Röbber, A. N. Bogdanov, C. Pfeleiderer, Spontaneous skyrmion ground states in magnetic metals, Nature 442 (2006) 797–801. doi:10.1038/nature05056.
- [6] N. A. Usov, S. E. Peschany, Magnetization curling in a fine cylindrical particle, J. Magn. Magn. Mater. 118 (3) (1993) L290–L294. doi:10.1016/0304-8853(93)90428-5.
- [7] K. L. Metlov, Magnetization patterns in ferromagnetic nano-elements as functions of complex variable, Phys. Rev. Lett. 105 (10) (2010) 107201. doi:10.1103/PhysRevLett.105.107201.
- [8] W. Doring, Point Singularities in Micromagnetism, J. Appl. Phys. 39 (2) (1968) 1006–1007. doi:10.1063/1.1656144.
- [9] L. D. Faddeev, Quantization of solitons, preprint IAS Print-75-QS70 (1975).
- [10] H. Hopf, Über die Abbildungen der dreidimensionalen Sphäre auf die Kugelfläche, Mathematische Annalen 104 (1) (1931) 637–665. doi:10.1007/BF01457962.
- [11] J. H. C. Whitehead, An Expression of Hopf’s Invariant as an Integral, Proceedings of the National Academy of Sciences 33 (5) (1947) 117–123. doi:10.1073/pnas.33.5.117.
- [12] D. A. Nicole, Solitons with non-vanishing Hopf index, Journal of Physics G: Nuclear Physics 4 (9) (1978) 1363–1369. doi:10.1088/0305-4616/4/9/008.
- [13] F. N. Rybakov, N. S. Kiselev, A. B. Borisov, L. Döring, C. Melcher, S. Blügel, Magnetic hopfions in solids, APL Materials 10 (11) (2022) 111113. arXiv:https://pubs.aip.org/aip/apm/article-pdf/doi/10.1063/5.0099942/16491966/111113\1_online.pdf, doi:10.1063/5.0099942. URL <https://doi.org/10.1063/5.0099942>

- [14] M. Sallermann, H. Jónsson, S. Blügel, Stability of hopfions in bulk magnets with competing exchange interactions, *Phys. Rev. B* 107 (2023) 104404. doi:10.1103/PhysRevB.107.104404.
URL <https://link.aps.org/doi/10.1103/PhysRevB.107.104404>
- [15] I. E. Dzyloshinskii, B. A. Ivanov, Localized topological solitons in a ferromagnet, *JETP Lett.* 29 (9) (1979) 540–542.
- [16] A. M. Kosevich, B. A. Ivanov, A. S. Kovalev, Magnetic solitons, *Phys. Rep.* 194 (3–4) (1990) 117–238. doi:10.1016/0370-1573(90)90130-T.
- [17] A. B. Borisov, V. Kiselev, *Topological Solitons, Two- and Three-Dimensional Patterns*, Vol. 2, UB Press of RAS, Ekaterinburg, 2011.
- [18] P. Sutcliffe, Hopfions in chiral magnets, *Journal of Physics A: Mathematical and Theoretical* 51 (37) (2018) 375401. doi:10.1088/1751-8121/aad521.
URL <https://dx.doi.org/10.1088/1751-8121/aad521>
- [19] Y. Liu, R. K. Lake, J. Zang, Binding a hopfion in a chiral magnet nanodisk, *Physical Review B* 98 (17) (Nov. 2018). doi:10.1103/physrevb.98.174437.
URL <http://dx.doi.org/10.1103/PhysRevB.98.174437>
- [20] N. Kent, N. Reynolds, D. Raftrey, I. T. G. Campbell, S. Virasawmy, S. Dhuey, R. V. Chopdekar, A. Hierro-Rodriguez, A. Sorrentino, E. Pereiro, S. Ferrer, F. Hellman, P. Sutcliffe, P. Fischer, Creation and observation of Hopfions in magnetic multilayer systems, *Nature Communications* 12 (1) (Mar. 2021). doi:10.1038/s41467-021-21846-5.
URL <http://dx.doi.org/10.1038/s41467-021-21846-5>
- [21] S. Castillo-Sepúlveda, R. M. Corona, E. Saavedra, D. Laroze, A. P. Espejo, V. L. Carvalho-Santos, D. Altbir, Nucleation and Stability of Toron Chains in Non-Centrosymmetric Magnetic Nanowires, *Nanomaterials* 13 (12) (2023). doi:10.3390/nano13121816.
URL <https://www.mdpi.com/2079-4991/13/12/1816>
- [22] F. Zheng, N. S. Kiselev, F. N. Rybakov, L. Yang, W. Shi, S. Blügel, R. E. Dunin-Borkowski, Hopfion rings in a cubic chiral magnet, *Nature* 623 (7988) (2023) 718–723. doi:10.1038/s41586-023-06658-5.
URL <http://dx.doi.org/10.1038/s41586-023-06658-5>

- [23] K. L. Metlov, Two types of metastable hopfions in bulk magnets, *Physica D* 443 (2023) 133561. doi:10.1016/j.physd.2022.133561.
- [24] V. G. Baryakhtar, E. P. Stefanovsky, Spin wave spectrum in antiferromagnets having a spiral magnetic structure, *Sov. Phys. Solid State* 11 (7) (1970) 1566–1572.
- [25] P. Bak, M. H. Jensen, Theory of helical magnetic structures and phase transitions in MnSi and FeGe, *J. Phys. C* 13 (31) (1980) L881–L885. doi:10.1088/0022-3719/13/31/002.
- [26] A. Aharoni, Introduction to the theory of ferromagnetism, Oxford University Press, Oxford, 1996.
- [27] M. Garst, J. Waizner, D. Grundler, Collective spin excitations of helices and magnetic skyrmions: review and perspectives of magnonics in non-centrosymmetric magnets, *J. Phys. D* 50 (29) (2017) 293002. doi:10.1088/1361-6463/aa7573.
- [28] R. M. M. Mattheij, G. W. M. Staarink, An Efficient Algorithm for Solving General Linear Two-Point BVP, *SIAM Journal on Scientific and Statistical Computing* 5 (4) (1984) 745–763. doi:10.1137/0905053.
- [29] K. L. Metlov, Source code, <https://github.com/metlov/magnhopf> (2024).
- [30] A. Bogdanov, D. Yablonskii, Thermodynamically stable "vortices" in magnetically ordered crystals. The mixed state of magnets, *Sov. Phys. JETP* 68 (1989) 101.
- [31] A. Bogdanov, A. Hubert, Thermodynamically stable magnetic vortex states in magnetic crystals, *J. Magn. Magn. Mater.* 138 (3) (1994) 255–269. doi:10.1016/0304-8853(94)90046-9.
- [32] K. L. Metlov, Simple analytical description of the cross-tie domain wall structure, *Appl. Phys. Lett.* 79 (16) (2001) 2609–2611. doi:10.1063/1.1409946.
- [33] C. Donnelly, K. L. Metlov, V. Scagnoli, M. Guizar-Sicairos, M. Holler, N. S. Bingham, J. Raabe, L. J. Heyderman, N. Cooper, S. Gliga, Experimental Observation of Vortex Rings in a Bulk Magnet, *Nat. Phys.*

17 (3) (2021) 316–321. arXiv:\protect\vrulewidth0pt\protect\
href{http://arxiv.org/abs/2009.04226}{arXiv:2009.04226},
doi:10.1038/s41567-020-01057-3.